

Periodic Asynchrony: An On-Policy Approach for Accelerating LLM Reinforcement Learning

Jian Lu

Big Data & AI Lab, Industrial and Commercial Bank of China (ICBC)

janelu@live.cn

Abstract

Since the introduction of the GRPO algorithm, reinforcement learning (RL) has attracted increasing attention for LLM post-training, yet training efficiency remains a critical challenge. In mainstream RL frameworks, inference and training are co-located on the same devices, and their synchronous execution prevents concurrent inference and training. In this work, we revisit the strategy of separating inference and training deployment, and propose a periodically asynchronous framework that transforms synchronous RL training into an asynchronous producer-consumer pipeline. Unlike existing asynchronous approaches that introduce off-policy bias, our design is provably equivalent to its synchronous counterpart, preserving strict on-policy correctness without any algorithmic modifications. We further introduce a unified tri-model architecture and a shared-prompt attention mechanism to support efficient asynchronous execution and reduce redundant computation. Experiments on NPU platforms demonstrate a three- to five-fold improvement in end-to-end training throughput over mainstream RL frameworks, while maintaining fully comparable accuracy, indicating its potential for widespread application.

1 Introduction

Reinforcement learning (RL) has re-emerged as a key technique for post-training and aligning large language models (LLMs). Following the introduction of GRPO by DeepSeek-R1 [Guo *et al.*, 2025], RL has demonstrated strong potential in improving reasoning capabilities, sparking growing interest in efficient RL pipelines across academia and industry.

Despite these advances, RL for LLMs still faces severe efficiency challenges. The training pipeline requires multiple models in the forward pass—the policy model, old-policy model, and reference model, and in some cases a value and reward model [Schulman *et al.*, 2017]—leading to substantial computational overhead. Moreover, each training step typically depends on generating large numbers of chain-of-thought (CoT) [Wei *et al.*, 2022] trajectories using the latest

policy weights, further increasing inference cost and memory usage.

To improve efficiency, early systems such as DeepSpeed-Chat [Yao *et al.*, 2023] relied on ZeRO-based distributed training, where the policy model handled inference directly, resulting in limited throughput. Later approaches decoupled training and inference, leveraging inference engines like vLLM [Kwon *et al.*, 2023] to accelerate rollout generation, as demonstrated by Open-R1 [Hugging Face, 2025]. Industry systems such as OpenRLHF [Hu *et al.*, 2024] push this further through training-inference co-location, although task switching still prevents full concurrency and independent scalability. Meanwhile, frameworks such as MindSpeed-RL [Feng *et al.*, 2025] and VERL [Sheng *et al.*, 2024] improve the training side through Megatron-style 3D parallelism [Shoeybi *et al.*, 2019].

Motivated by these limitations, we revisit the training-inference separation strategy and introduce a synchronous framework enhanced with new system-level optimizations. Our design uses a Megatron-style 3D parallel backbone and adds a background producer process that continuously dispatches prompts to inference workers, while the main consumer process retrieves outputs and performs training. Samples from each group are split into micro-batches and trained sequentially, and model weights are synchronized only after the full batch is consumed. This *periodic asynchrony* achieves purely on-policy asynchronous acceleration and is compatible with any on-policy RL algorithm. The decoupled architecture enables flexible scaling of inference workers, avoiding inference bottlenecks, and for GRPO, we further introduce a shared-prompt attention mask to eliminate redundant computation. Experiments on NPU platforms show that our proposed framework achieves a three- to five-fold improvement in end-to-end training throughput over mainstream RL frameworks, with near-linear scaling as the number of devices increases.

2 Related Work

Improving the efficiency of reinforcement learning (RL) for large language models (LLMs) has attracted increasing attention across academia and industry. Although synchronous frameworks dominate large-scale RL systems due to their stability, they often underutilize computational resources. To address this, recent studies explore asynchronous training

paradigms that decouple inference from training to enhance throughput and scalability. We review representative efforts, with emphasis on asynchronous RL methods.

An early attempt is Asynchronous RLHF [Noukhovitch *et al.*, 2024], which decouples generation and learning so that new sample generation and old-sample training proceed in parallel. Its key idea is online but off-policy RLHF, updating models with samples from previous iterations. While effective, it remains a typical off-policy strategy and is less suitable for strictly on-policy algorithms such as GRPO, especially in long-context settings.

Most recently, AReAL [Fu *et al.*, 2025] advances asynchronous RL for LLM reasoning by fully decoupling generation from training and introducing explicit staleness control through a parameter η . To tolerate delayed samples, it adopts a staleness-aware PPO variant that relaxes the strict on-policy assumption. While effective in improving training efficiency, this design modifies standard on-policy objectives and introduces controlled bias, whose generalization across algorithms and data regimes remains theoretically unclear. In parallel, several recent works focus on system-level asynchrony to improve the scalability of LLM post-training. ROLL Flash [Lu *et al.*, 2025], Lamina [Sheng *et al.*, 2025], and LlamaRL [Wu *et al.*, 2025] propose fully decoupled asynchronous execution frameworks that eliminate global synchronization barriers and maximize throughput under variable rollout latency. Trajectory Balance with Asynchrony [Bartoldson *et al.*, 2025] further explores decoupling exploration and learning to accelerate post-training. These systems primarily address efficiency from a systems perspective and typically rely on standard PPO-style updates, without explicitly constraining policy staleness or preserving strict on-policy correctness.

These fully asynchronous designs effectively trade a degree of on-policy correctness for throughput, preventing transient blocking between inference and learning. Although their experiments demonstrate the effectiveness of this approach, whether it generalizes across all RL algorithms and data regimes remains theoretically unproven.

In contrast, our method takes a complementary algorithmic perspective: we propose a periodically asynchronous framework that preserves strict on-policy correctness without algorithmic modifications, while introducing a unified tri-model architecture and shared-prompt attention mechanism to further improve system efficiency. Unlike existing asynchronous approaches, our design is provably equivalent to synchronous training, offering theoretical guarantees that generalize across on-policy RL algorithms.

3 Background

Training RL with Micro-Batching

We first establish that micro-batch training is mathematically compatible with on-policy RL objectives, as this forms the theoretical foundation for the gradient accumulation scheme used in our asynchronous framework.

In distributed large-scale training, micro-batching is a standard technique that partitions a full batch into smaller micro-batches, accumulating gradients across micro-steps before each parameter update. This is mathematically equivalent to

full-batch training while avoiding out-of-memory errors. We extend this equivalence to RL and show it holds for GRPO.

The GRPO objective for a single prompt with G sampled responses is:

$$J_{\text{GRPO}}(\theta) = \frac{1}{G} \sum_{i=1}^G \left(L_i(\pi_\theta \| \pi_{\text{old}}, A_i) - \beta D_{KL}^i(\pi_\theta \| \pi_{\text{ref}}) \right), \quad (1)$$

where the PPO-style clipped advantage term is defined as:

$$L_i(\pi_\theta \| \pi_{\text{old}}, A_i) = \min \left(\frac{\pi_\theta(o_i|q)}{\pi_{\text{old}}(o_i|q)} A_i, \text{clip} \left(\frac{\pi_\theta(o_i|q)}{\pi_{\text{old}}(o_i|q)}, 1 - \varepsilon, 1 + \varepsilon \right) A_i \right), \quad (2)$$

and the KL divergence penalty is:

$$D_{KL}^i(\pi_\theta \| \pi_{\text{ref}}) = \frac{\pi_{\text{ref}}(o_i|q)}{\pi_\theta(o_i|q)} - \log \frac{\pi_{\text{ref}}(o_i|q)}{\pi_\theta(o_i|q)} - 1. \quad (3)$$

For a training batch of N prompts, the batch-level objective aggregates over all NG response samples:

$$J_{\text{batch}} = \frac{1}{N} \sum_{i=1}^N J_{\text{GRPO}}^i = \frac{1}{NG} \sum_{k=1}^{NG} \left(L_k - \beta D_{KL}^k \right). \quad (4)$$

Partitioning the NG samples into $M = \lfloor NG/m \rfloor$ micro-batches of size m , the objective decomposes as:

$$J_{\text{batch}} = \frac{1}{M} \sum_{i=1}^M \frac{1}{m} \sum_{j=1}^m \left(L_{i,j} - \beta D_{KL}^{i,j} \right), \quad (5)$$

which is mathematically equivalent to the full-batch update. This confirms that GRPO training is fully compatible with micro-batching: although each batch now contains NG samples rather than N , memory consumption remains bounded by the micro-batch size m , enabling reinforcement learning over sequences as long as those supported in supervised fine-tuning. This property is directly exploited in our asynchronous framework, where samples arriving from the inference queue are accumulated as micro-batches and trained sequentially without waiting for the full batch to complete.

4 System Design

4.1 System Overview

When performing reinforcement learning with large-scale models using different frameworks for inference and training—for instance, vLLM for inference and Megatron for training—the process generally involves three main steps:

1. Synchronize the weights of the policy model with the inference engine.
2. The inference engine retrieves prompts from the dataloader and generates responses. A reward module evaluates these responses based on the corresponding prompts, distinguishing high-quality outputs from lower-quality ones.

- The generated samples and their associated scores are then sent to the training engine, which computes the loss and performs backpropagation to update the policy model parameters.

For the third step, mainstream reinforcement learning systems typically require the computation of three types of logits in the forward pass: policy, old policy, and reference. These models share the same architecture, differing only in their weights. How these three models are organized and distributed in our system will be detailed in Section 4.2, as their design is closely tied to the requirements of asynchronous execution.

4.2 Periodic Asynchronous Reinforcement Learning

Asynchronous execution of inference and training is a key factor in accelerating reinforcement learning systems with a separated training-inference architecture. In such asynchronous systems, the critical aspect is minimizing the time the training engine waits for the rollout workers to return generated samples, i.e., the startup latency. In this work, we propose a simple approach that introduces a temporary data generator between the data loader and the trainer. This design transforms on-policy reinforcement learning from synchronous to asynchronous execution, significantly improving training efficiency without requiring any modifications to the underlying reinforcement learning algorithm.

Asynchronous Execution Mechanism

The reinforcement learning workflow incorporating the temporary sample generator is illustrated in Figure 1. It follows a typical *producer-consumer* pattern and consists of four main components:

- Data source**, which is the original data loader.
- Temporary data generator**, the additional component introduced in this work, which includes a background thread acting as a producer and a queue shared with the main process.
- Inference service**, responsible for receiving prompts and generating responses.
- Trainer**, which consumes the samples from the queue for training.

The core of our asynchronous design lies in the operation of the temporary generator. Within the temporary generator, a batch of prompts required for one training step is first retrieved from the standard data loader. A background thread is then launched to act as a *producer*. Inside this thread, a coroutine is used to concurrently and evenly dispatch the entire batch of prompts to multiple inference instances within the inference service. Upon receiving a large number of requests, the inference instances efficiently generate responses through continuous batching and return the completed responses back to the coroutine.

To fully exploit coroutine-level parallelism, the reward function is integrated directly into the coroutine. Each response returned by an inference instance is immediately

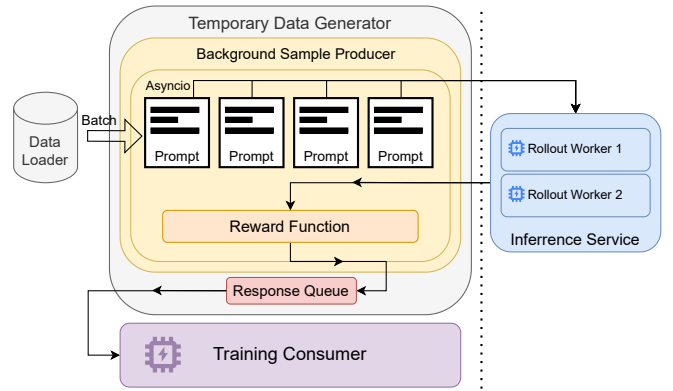


Figure 1: Operational Mechanism of the Asynchronous System.

scored, and once both inference and evaluation for a coroutine’s assignment are finished, the resulting responses and reward scores are placed into a queue shared with the main process. This queue serves as a buffer that temporarily stores the generated responses from inference service.

The main process, acting as the *consumer*, continuously retrieves completed samples from the queue and feeds them to the training engine. Under this design, the start time of training is determined by the earliest completed sample among all prompts in the batch. Once all prompts in the batch have been processed, the inference service enters an idle state until the training step finishes and the updated policy weights are synchronized back to the rollout workers. Only then does the next training cycle begin. Therefore, we refer to this design as **periodic asynchrony**.

As implied by the consumer-side design, each training step requires the simultaneous computation of three types of logits—policy, old policy, and reference—for every consumed sample. To address this, we adopt a unified tri-model architecture in which all three models share an identical parallel layout across computational units, implemented on a Megatron-like backbone distributed according to tensor parallelism and pipeline parallelism scales. Each sub-network is replicated twice—once for the old policy logits and once for the reference logits—where the reference network retains the original model weights and the old policy network holds weights delayed by one training step.

As illustrated in Figure 2, this shared distribution allows the logits of all three models to be computed simultaneously in a single micro-step. After all samples in a batch complete their forward passes, the policy model’s current weights are moved into the old policy model’s `state_dict` before the next parameter update. This design ensures consistent and well-defined weight synchronization at every update boundary, serving as a structural prerequisite for the correctness of the periodic asynchronous framework. Furthermore, since all three models share the same parallel topology, their computational resources are managed uniformly, eliminating the need for separate resource allocation and scheduling across model types and further simplifying system design.

The complete procedure is summarized in Algorithm 1.

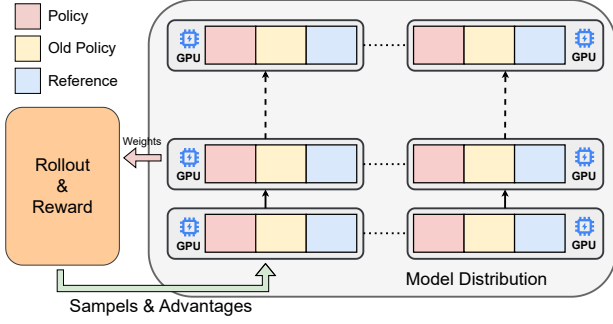


Figure 2: Triple Models with Shared Distribution.

Algorithm 1 Periodic Asynchronous Reinforcement Learning Algorithm

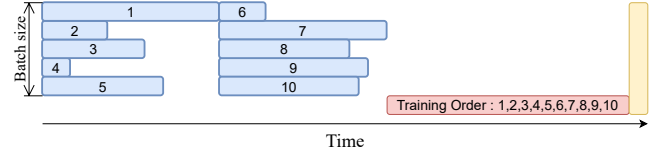
Input: Dataloader D , training iterations T , batch size B

Output: Trained policy model

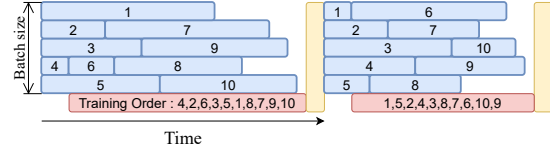
- 1: Initialize shared queue Q and gradient accumulator O
 - 2: **for** $t = 1$ to T **do**
 - 3: Synchronize policy model weights to the rollout workers
 - 4: Retrieve prompts $P = \{p_1, \dots, p_B\}$ from D
 - 5: **Producer thread:**
 - 6: Create B concurrent coroutine tasks
 - 7: **Run in parallel for each** $i = 1, \dots, B$:
 - 8: $r_i \leftarrow \text{InferenceService}(p_i)$
 - 9: $a_i \leftarrow \text{RewardFunction}(r_i)$
 - 10: Enqueue (a_i, r_i) into Q
 - 11: $O \leftarrow 0$
 - 12: $\text{consumed_count} \leftarrow 0$
 - 13: **while** $\text{consumed_count} < B$ **do**
 - 14: $(a_i, r_i) \leftarrow \text{Dequeue}(Q)$
 - 15: $s_i \leftarrow \text{ProcessSample}(p_i, r_i)$
 - 16: Compute loss $L(s_i)$ and gradient $\nabla L(s_i)$
 - 17: $O \leftarrow O + \nabla L(s_i)$
 - 18: $\text{consumed_count} \leftarrow \text{consumed_count} + 1$
 - 19: **end while**
 - 20: Move policy’s weights into old-policy’s modules
 - 21: Update policy’s weights with accumulated gradient O
 - 22: **end for**
-

Efficiency Analysis

Figure 3a and Figure 3b illustrate the differences between the asynchronous training system studied in this paper and a synchronous training system. It is evident that in a synchronous system, the training process must wait for all prompts to be processed by the inference service. If the batch size is large, multiple inference batches may be required to complete all the prompts. The startup time for training is determined by the inference batches and the sum of the inference times of the slowest samples in each batch. Assuming the inference engine has a batch size of m and the prompts of one training batch are divided into n inference batches, the training startup time can be expressed as:



(a) Synchronous training step.



(b) Asynchronous two-step training.

Legend: Inference (blue), Training (red), Update Weight (yellow)

Figure 3: Comparison of synchronous vs. asynchronous training.

$$T_{sync} = \sum_{j=0}^n \max \{t_j^i | i \in \{0, 1, \dots, m\}\} \quad (6)$$

Where t_j^i denotes the time required for the i -th prompt in the j -th batch to complete inference. In contrast, for an asynchronous system, the training startup time depends only on the earliest-completed prompt in the first inference batch, which can be expressed as:

$$T_{async} = \min \{t_i^0 | i \in \{0, 1, \dots, m\}\} \quad (7)$$

After that, all samples in the batch are trained sequentially in the order in which they enter the queue. It is clear that when inference speed and training speed are well balanced, the sum of their waiting times is minimized, resulting in optimal end-to-end training throughput on a given hardware configuration. Therefore, in theory, the asynchronous system can achieve nearly twice the end-to-end training speed of the synchronous system. Although in rare extreme cases the training time of a single step may be dominated entirely by either inference or training alone, such imbalance can be mitigated through complementary optimizations—for instance, the shared-prompt attention mechanism introduced in Section 4.3 effectively reduces training computation, and the decoupled inference–training architecture naturally enables load balancing by allowing independent scaling of inference and training instances.

Correctness Analysis

As shown in Figure 3b, the asynchronous system trains samples in a different order from the synchronous system, determined by inference completion time rather than the original batch order. We now formally establish that neither the on-policy correctness nor the gradient equivalence is compromised by this reordering.

Proposition 1 (Periodic Weight Consistency). *All rollout samples within the same batch are generated by the same policy π_{θ_t} , i.e.:*

$$\forall i \in \{1, \dots, B\} : o_i \sim \pi_{\theta_t}(\cdot | p_i). \quad (8)$$

Proof. Line 3 synchronizes all inference workers to θ_t before any rollout begins, and no weight update is performed until Line 21, after all B samples have been consumed. Therefore, every o_i is sampled exclusively from π_{θ_t} , satisfying the on-policy condition identically to a synchronous system.

Having established on-policy sample consistency, we next show that the order in which these samples are consumed during training does not affect the gradient update.

Proposition 2 (Gradient Permutation Invariance). *Let σ be any permutation of the NG training samples across micro-batches. The accumulated gradient is invariant to σ :*

$$\nabla_{\theta} J_{\text{batch}} = \frac{1}{NG} \sum_{k=1}^{NG} \nabla_{\theta} \left(L_k - \beta D_{KL}^k \right). \quad (9)$$

Proof. The double summation $\sum_{i=1}^M \sum_{j=1}^m$ enumerates all NG samples regardless of their ordering. The result follows directly from the commutativity of finite summation.

This guarantees that the periodic asynchronous system is algorithmically equivalent to its synchronous counterpart, with any on-policy RL algorithm remaining correct under asynchronous execution without modification. Combining Proposition 1 and Proposition 2, we arrive at the main theorem of this section.

Theorem 1 (Equivalence of Asynchronous and Synchronous Updates). *At each training iteration t , the periodic asynchronous system produces an identical parameter update to its synchronous counterpart:*

$$\Delta \theta_{\text{async}}^t = \Delta \theta_{\text{sync}}^t. \quad (10)$$

Consequently, the two systems follow exactly the same training trajectory $\{\theta_t\}$, confirming that periodic asynchrony is purely on-policy and algorithmically equivalent to synchronous RL training.

We can thus conclude that the proposed periodic asynchronous framework constitutes a fully on-policy asynchronous reinforcement learning system that is algorithmically decoupled from the underlying RL algorithm, requiring no modifications to ensure correct operation. Its convergence and stability are identical to those of any synchronous on-policy method it is built upon.

4.3 Shared-Prompt Attention

In GRPO-based reinforcement learning, all samples within a group are generated from the same prompt, making it possible to share the prompt computation across responses within a micro-batch, which significantly reduces redundant computation and memory consumption when prompts are long relative to responses.

Compared with standard training, the shared-prompt approach introduces four targeted modifications to the input construction, positional encoding, attention mask, and loss computation respectively:

1. Concatenate the shared prompt with the token IDs of multiple responses. The corresponding labels are concatenated accordingly, while the prompt portion is excluded from the labels.

$$\begin{cases} x = [x_p, x_{r_1}, x_{r_2}] \\ y = [y_{r_1}, y_{r_2}] \end{cases} \quad (11)$$

where x_p denotes the token IDs of the shared prompt, and x_{r_1}, x_{r_2} correspond to the tokens of the individual responses.

2. Rearrange the position indices such that each response starts immediately after the prompt, ensuring positional continuity with the shared prompt.

$$p = (0, 1, \dots, |x_p| - 1, |x_p|, \dots, |x_p| + |x_{r_1}| - 1, |x_p|, \dots, |x_p| + |x_{r_2}| - 1) \quad (12)$$

where $|\cdot|$ denotes sequence length.

3. In the attention module, a shared-prompt mask (Figure 4) is used instead of the standard causal mask. This design restricts each response token to attend only to the shared prompt, preventing information leakage across responses.

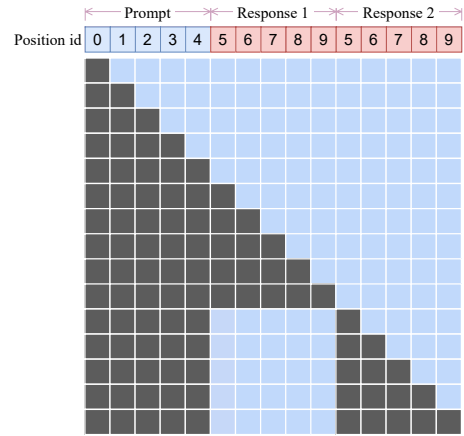


Figure 4: Shared-prompt attention mask.

4. For probability computation, the prompt tokens are discarded and the loss is computed only over the response tokens:

$$\pi = -\text{CrossEntropy}(\hat{y}_{|x_p|:|x|}, y), \quad (13)$$

where $\hat{y}_{|x_p|:|x|}$ represents the predicted logits of the response tokens.

Correctness Analysis. By construction of the shared-prompt mask (Step 3), each response token attends only to the prompt and its own preceding tokens, with cross-response attention fully masked. Therefore, the hidden states and gradients of each response are determined solely by x_p and x_{r_k} , giving:

$$\nabla_{\theta} \mathcal{L}_{\text{shared}} = \sum_{k=1}^K \nabla_{\theta} \mathcal{L}_k, \quad (14)$$

where \mathcal{L}_k denotes the loss on the k -th response under standard training. This confirms that the shared-prompt approach is mathematically equivalent to standard per-sample training, introducing no approximation or bias into the training objective.

Complexity Analysis. Let L_p , L_r , and K denote the prompt length, average response length, and number of responses per micro-batch, respectively. In standard training, the prompt tokens are redundantly computed K times, giving a total attention complexity of $\mathcal{O}(K(L_p + L_r)^2)$. Under the shared-prompt approach, the attention computation decomposes into three parts according to the mask structure: prompt self-attention $\mathcal{O}(L_p^2)$, response-to-prompt attention $\mathcal{O}(KL_rL_p)$, and response self-attention $\mathcal{O}(KL_r^2)$, giving a total of $\mathcal{O}(L_p^2 + KL_r(L_p + L_r))$. The reduction ratio between the two approaches is:

$$\rho = \frac{L_p^2 + KL_r(L_p + L_r)}{K(L_p + L_r)^2} \quad (15)$$

When $L_p \gg L_r$, ρ approaches $\frac{1}{K}$, yielding an approximately K -fold reduction in attention computation. Additionally, no padding is required for shorter responses within a micro-batch, further improving hardware utilization. These gains are therefore most pronounced in long-prompt, short-response settings, which are common in complex reasoning tasks with GRPO.

5 Implementation

Our implementation is built on the **PyTorch** training framework, using a 3D-parallel distributed architecture. We incorporate parts of Megatron-Core and DeepSpeed [Rasley *et al.*, 2020]. On the **NPU** platform, we additionally use MindSpeed, `torch_npu`, and optimized operators such as `npu_fusion_attention`, an accelerated attention kernel supporting custom masks and serving as a counterpart to `flash_attention` [Dao, 2023]. For inference, we use **vLLM**, with `ascend_vLLM` on NPUs.

As in fine-tuning, all RL samples are computed at their native sequence lengths for both forward and backward passes without padding, following dynamic-length training. The inference-to-training instance ratio is configurable and set to 1:4 in all experiments, chosen to balance inference and training throughput on the Ascend-910B platform.

All components described above are publicly available in project release v5.0.5 (September 5, 2025) at <https://github.com/janelu9/EasyLLM>.

6 Experiments

We evaluate four reinforcement learning frameworks on mathematical reasoning tasks: MindSpeed-RL, an official NPU training framework using a Megatron backend with shared-accelerator design; VERL, a mainstream framework using an FSDP backend with asynchronous execution; our synchronous baseline under a decoupled training-inference design; and our proposed asynchronous framework. The primary evaluation metric is end-to-end training throughput, measured by tokens trained per second per device (TPSPD). Accuracy metrics are provided as reference to verify that no degradation is introduced by our algorithmic design.

6.1 Model and Environment Configuration

The models compared in this section are Qwen2.5-7B-Instruct [Team and others, 2024], Qwen3-8B [Yang *et al.*,

2025], and DeepSeek-R1-Distill-Qwen-32B [DeepSeek-AI, 2025]. The training data comes from the publicly available math problem datasets DeepScaleR [Luo and others, 2025] and GSM8K [Cobbe *et al.*, 2021]. All reinforcement learning experiments use the GRPO algorithm. The accuracy test set is AIME24 [Zhang and Math-AI, 2024].

Experiments were conducted on **air-cooled** Ascend-910B NPUs, with each node equipped with eight 64 GB NPUs. The intra-node interconnect bandwidth is 196 GB/s, and the inter-node bandwidth is 100 Gb/s.

6.2 Training Throughput Comparison

Comparison with Existing Frameworks

8B Model on DeepScaleR. Table 1 reports results for Qwen3-8B trained on DeepScaleR with a 16K context length. Since prompts in this dataset are significantly shorter than responses, *Shared-Prompt Attention* is disabled for all methods in this experiment. Our asynchronous framework achieves a TPSPD of 192.259, outperforming MindSpeed-RL ($3.12\times$), VERL ($1.24\times$), and our synchronous baseline ($1.92\times$). The $1.92\times$ speedup over the synchronous baseline is particularly noteworthy, as it closely approaches the theoretical upper bound of $2\times$ derived in Section 4.2, validating the efficiency analysis of the periodic asynchronous framework in a practical setting.

32B Model on DeepScaleR. Table 2 reports results for DeepSeek-R1-Distill-Qwen-32B. In the first group, our asynchronous framework running on only 48 NPUs achieves a TPSPD of 33.449, delivering a $5.05\times$ speedup over MindSpeed-RL running on 64 NPUs. This result is particularly significant: not only does our method achieve substantially higher throughput, it does so with fewer hardware resources, demonstrating both efficiency and resource economy. In the second group, all frameworks are evaluated at 8K context to align with VERL, which encounters out-of-memory issues at 16K. VERL’s accuracy drops sharply to 0.617—well below the base model level—while our framework maintains 0.675, a degradation we attribute to response truncation at insufficient context length. Our asynchronous framework achieves a further $1.76\times$ speedup over VERL even under these favorable conditions for VERL.

7B Model on GSM8K. Table 3 studies the training-dominated regime using Qwen2.5-7B-Instruct on GSM8K with a 1K context. Our asynchronous framework with *Shared-Prompt Attention* enabled achieves a TPSPD of 435.596, the highest among all settings, corresponding to a $2.19\times$ speedup over MindSpeed-RL and $2.39\times$ over VERL. Notably, both competing frameworks also achieve competitive accuracy, confirming that the throughput gap is not due to shortcuts in training quality.

Architectural Analysis

To isolate the contribution of our architectural design from the benefit of asynchronous execution, we compare *Sync (ours)* directly against MindSpeed-RL, the strongest competing synchronous framework. Under identical synchronous execution, our framework achieves a $1.62\times$ speedup on the 8B model (Table 1) and a $3.96\times$ speedup on the 32B model

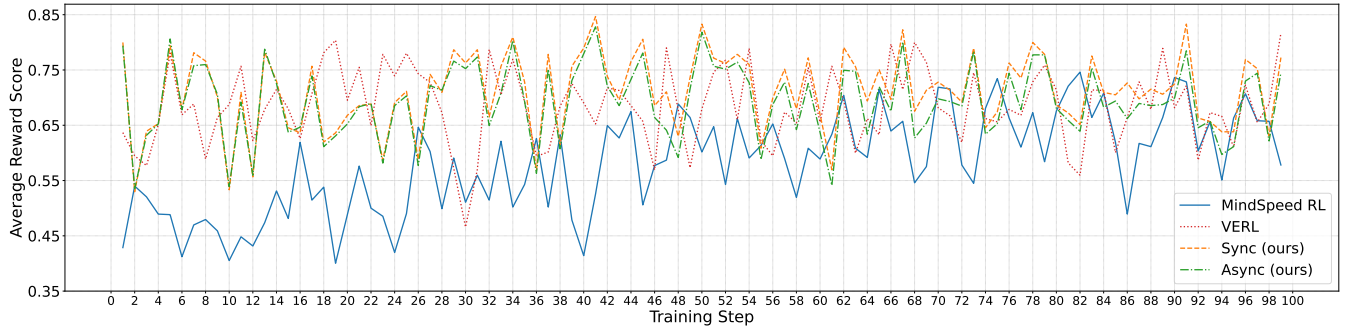


Figure 5: Training step-wise average reward score comparison.

Setting	AIME24	Micro-BS	Training Tokens	TPSPD
Base model (8B)	0.725	–	–	–
MindSpeed-RL	0.733	1	706.355 M	61.641
VERL (async)	0.746	16	812.084 M	155.521
Sync (ours)	0.746	1	827.306 M	99.966
Async (ours)	0.758	1	917.609 M	192.259

Table 1: All frameworks are trained for 100 steps using 16 NPUs with a global batch size of 32. For GRPO, each group performs 32 rollouts. Since VERL adopts an FSDP backend, the micro-batch size is set to at least 16 and its asynchronous execution is enabled.

Setting	AIME24	NPUs	GBS	MBS	Training Tokens	TPSPD
Base model (32B)	0.696	–	–	–	–	–
MindSpeed-RL	0.717	64	32	1	107.874 M	6.627
Sync (ours)	0.725	48	32	1	123.613 M	26.219
Async (ours)	0.738	48	32	1	123.999 M	33.449
VERL (async)	0.617	64	64	64	157.765 M	44.016
Sync (ours)	0.700	64	64	1	185.796 M	46.519
Async (ours)	0.675	64	64	1	188.081 M	77.342

Table 2: All frameworks are trained for 20 steps. For GRPO, each group performs 32 rollouts. In the additional group of experiments, the global batch size (GBS) is increased to 64, since VERL requires a minimum micro-batch size (MBS) of 64 when running on 64 NPUs. VERL is evaluated at 8K context due to out-of-memory issues at 16K.

Setting	GSM8K	Micro-BS	Training Tokens	TPSPD
Base model (7B)	0.801	–	–	–
MindSpeed-RL	0.890	16	72.534 M	199.142
VERL (async)	0.869	16	90.042 M	182.560
Async (ours), w/o SPA	0.912	1	84.192 M	54.463
Sync (ours), w/ SPA	0.930	16	60.586 M	218.396
Async (ours), w/ SPA	0.919	16	60.926 M	435.596

Table 3: All frameworks are trained on 16 NPUs and complete training on the full GSM8K training set at step 116. For GRPO, each group performs 32 rollouts, and the context length is fixed to 1K for all settings. SPA denotes *Shared-Prompt Attention*. A micro-batch size of 1 indicates SPA is disabled, whereas 16 means 16 rollouts share a single prompt. Evaluation is conducted on the GSM8K test set.

(Table 2), attributable to the efficiency of the decoupled training–inference design and the unified tri-model architecture. Furthermore, in the training-dominated GSM8K setting, *Sync (ours)*, w/ SPA (TPSPD: 218.396) already surpasses *VERL (async)* (TPSPD: 182.560) despite using synchronous execution, demonstrating that *Shared-Prompt Attention* alone is sufficient to overcome the throughput gap in training-dominated regimes. These results confirm that the architectural contributions of this work provide independent and meaningful efficiency gains beyond asynchronous execution alone.

Ablation Analysis

Table 3 enables a clean ablation of the two key components proposed in this work: the periodic asynchronous framework and *Shared-Prompt Attention*. We isolate their respective contributions as follows.

Effect of Shared-Prompt Attention. Comparing *Async (ours)*, w/o SPA (TPSPD: 54.463) with *Async (ours)*, w/ SPA (TPSPD: 435.596) under otherwise identical settings reveals that enabling *Shared-Prompt Attention* alone yields an $8\times$ improvement in throughput. This gain stems from two sources: a reduction in training tokens from 84.192 M to 60.926 M due to shared prompt computation, and the elimination of padding overhead within micro-batches. These results are consistent with the K -fold complexity reduction predicted by the analysis in Section 4.3, where $K = 16$ rollouts share a single prompt.

Effect of Periodic Asynchrony. Comparing *Sync (ours)*, w/ SPA (TPSPD: 218.396) with *Async (ours)*, w/ SPA (TPSPD: 435.596) isolates the contribution of asynchronous execution under identical architecture and data conditions. The asynchronous framework delivers a $2\times$ speedup, closely matching the theoretical upper bound established in Section 4.2, and confirming that the overlap between inference and training is effectively exploited in practice.

Combined Effect. The two components are complementary in nature: *Shared-Prompt Attention* reduces the per-step training cost, while periodic asynchrony minimizes idle waiting time between inference and training. Together, they deliver a $2.19\times$ speedup over the strongest competing framework MindSpeed-RL and an $8\times$ speedup over our unoptimized baseline (*Async w/o SPA*), demonstrating that the ben-

efits of the two components are largely multiplicative.

Accuracy Validation

For accuracy evaluation, we employ a rule-based method where the predicted answer is considered correct if it can be accurately extracted and matches the ground-truth answer in the dataset; otherwise it is deemed incorrect. As shown across all tables, the accuracy of our framework remains consistent with competing methods, with differences falling within the expected range of random fluctuation. Furthermore, the reward trajectories of our synchronous and asynchronous methods almost completely overlap throughout training, as shown in Figure 5, empirically corroborating the theoretical equivalence established in Theorem 1. These results confirm that the substantial throughput gains introduced by our framework come at no cost to training effectiveness.

6.3 Scalability Analysis

We conduct a set of experiments to evaluate the scalability of our framework using the same configuration as the first experiment group. The results are shown in Table 4.

Model	NPUs	Training Steps	Tokens/Sec/Device
Qwen3-8B	16	20	188.162
	32	20	171.824
	64	20	163.208

Table 4: Scalability comparison results. TPSPD performance of training Qwen3-8B on 16, 32, and 64 NPUs using our asynchronous framework. The training-to-inference instance ratio is fixed at 1:4.

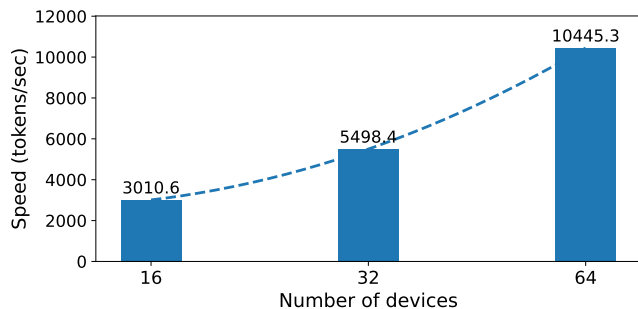


Figure 6: TPS of our framework under different data-parallel scales.

When expressed in TPS (tokens per second), the results are more intuitively illustrated in Figure 6. Training with 32 NPUs shows a $1.83\times$ speedup compared to 16 NPUs, while using 64 NPUs results in a $1.9\times$ speedup over 32 NPUs, demonstrating near-linear scaling in total throughput. The moderate decrease in TPSPD with increasing device count is expected, as inter-node communication overhead grows with scale while the training-to-inference ratio is held fixed at 1:4. Overall, the proposed asynchronous reinforcement learning framework demonstrates strong scalability as the number of devices increases.

7 Conclusion

This paper addresses the training efficiency bottleneck in on-policy reinforcement learning by proposing a periodically asynchronous framework that achieves provably equivalent updates to synchronous training. By introducing a temporary data generator between the data loader and the trainer, the framework transforms synchronous RL into an asynchronous producer-consumer pipeline, maximizing the overlap between inference and training without any algorithmic modifications. We theoretically establish that micro-batch training is fully compatible with on-policy RL objectives, and prove that neither the on-policy correctness nor the gradient equivalence is compromised by asynchronous execution. A unified tri-model architecture with identically distributed components is introduced to support efficient and consistent weight synchronization, along with a shared-prompt attention mechanism that significantly reduces redundant computation in long-prompt, short-response settings. Experimental results on NPU platforms demonstrate a three- to five-fold improvement in end-to-end throughput over mainstream RL frameworks, while maintaining fully comparable training effectiveness. Furthermore, the decoupling of training and inference enables independent and flexible scaling, and the algorithm-agnostic design ensures compatibility with any on-policy RL method, allowing the community to benefit from asynchronous acceleration without sacrificing theoretical guarantees.

References

- [Bartoldson *et al.*, 2025] Brian Bartoldson, Siddarth Venkaraman, James Diffenderfer, Moksh Jain, Tal Ben-Nun, Seanie Lee, Minsu Kim, Johan Obando-Ceron, Yoshua Bengio, and Bhavya Kailkhura. Trajectory balance with asynchrony: Decoupling exploration and learning for fast, scalable llm post-training, 2025.
- [Cobbe *et al.*, 2021] Karl Cobbe, Vineet Kosaraju, Mohammad Bavarian, Mark Chen, Heewoo Jun, Lukasz Kaiser, Matthias Plappert, Jerry Tworek, Jacob Hilton, Reiichiro Nakano, Christopher Hesse, and John Schulman. Training verifiers to solve math word problems. *arXiv preprint arXiv:2110.14168*, 2021.
- [Dao, 2023] Tri Dao. Flashattention-2: Faster attention with better parallelism and work partitioning. *arXiv preprint arXiv:2307.08691*, 2023.
- [DeepSeek-AI, 2025] DeepSeek-AI. Deepseek-r1: Incentivizing reasoning capability in llms via reinforcement learning, 2025.
- [Feng *et al.*, 2025] Laingjun Feng, Chenyi Pan, Xinjie Guo, Fei Mei, Benzhe Ning, Jianxiang Zhang, Xinyang Liu, Beirong Zhou, Zeng Shu, Chang Liu, Guang Yang, Zhenyu Han, Jiangben Wang, and Bo Wang. Mindspeed rl: Distributed dataflow for scalable and efficient rl training on ascend npu cluster, 2025.
- [Fu *et al.*, 2025] Wei Fu, Jiakuan Gao, Xujie Shen, Chen Zhu, Zhiyu Mei, Chuyi He, Shusheng Xu, Guo Wei, Jun Mei, Jiashu Wang, Tongkai Yang, Binhang Yuan, and

- Yi Wu. Areal: A large-scale asynchronous reinforcement learning system for language reasoning, 2025.
- [Guo *et al.*, 2025] Daya Guo, Dejian Yang, Haowei Zhang, Junxiao Song, Peiyi Wang, Qihao Zhu, Runxin Xu, Ruoyu Zhang, Shirong Ma, Xiao Bi, et al. Deepseek-r1 incentivizes reasoning in llms through reinforcement learning. *Nature*, 645(8081):633–638, 2025.
- [Hu *et al.*, 2024] Jian Hu, Xibin Wu, Zilin Zhu, Xianyu, Weixun Wang, Dehao Zhang, and Yu Cao. Openrlhf: An easy-to-use, scalable and high-performance rlhf framework. *arXiv preprint arXiv:2405.11143*, 2024.
- [Hugging Face, 2025] Hugging Face. Open r1: A fully open reproduction of deepseek-r1, January 2025.
- [Kwon *et al.*, 2023] Woosuk Kwon, Zhuohan Li, Siyuan Zhuang, Ying Sheng, Lianmin Zheng, Cody Hao Yu, Joseph E. Gonzalez, Hao Zhang, and Ion Stoica. Efficient memory management for large language model serving with pagedattention. In *Proceedings of the ACM SIGOPS 29th Symposium on Operating Systems Principles*, 2023.
- [Lu *et al.*, 2025] Han Lu, Zichen Liu, Shaopan Xiong, Yancheng He, Wei Gao, Yanan Wu, Weixun Wang, Jishun Liu, Yang Li, Haizhou Zhao, Ju Huang, Siran Yang, Xiaoyang Li, Yijia Luo, Zihe Liu, Ling Pan, Junchi Yan, Wei Wang, Wenbo Su, Jiamang Wang, Lin Qu, and Bo Zheng. Part ii: Roll flash – accelerating rlvr and agentic training with asynchrony, 2025.
- [Luo and others, 2025] Michael Luo et al. Deepscaler: Surpassing o1-preview with a 1.5b model by scaling rl. <https://tinyurl.com/deepscaler-2025>, 2025. Notion Blog.
- [Noukhovitch *et al.*, 2024] Michael Noukhovitch, Shengyi Huang, Sophie Xhonneux, Arian Hosseini, Rishabh Agarwal, and Aaron Courville. Asynchronous rlhf: Faster and more efficient off-policy rl for language models. *arXiv preprint arXiv:2410.18252*, 2024.
- [Rasley *et al.*, 2020] Jeff Rasley, Samyam Rajbhandari, Olatunji Ruwase, and Yuxiong He. DeepSpeed: System optimizations enable training deep learning models with over 100 billion parameters. In *Proceedings of the 26th ACM SIGKDD international conference on knowledge discovery & data mining*, pages 3505–3506, 2020.
- [Schulman *et al.*, 2017] John Schulman, Filip Wolski, Prfulla Dhariwal, Alec Radford, and Oleg Klimov. Proximal policy optimization algorithms. *arXiv preprint arXiv:1707.06347*, 2017.
- [Sheng *et al.*, 2024] Guangming Sheng, Chi Zhang, Zilingfeng Ye, Xibin Wu, Wang Zhang, Ru Zhang, Yanghua Peng, Haibin Lin, and Chuan Wu. Hybridflow: A flexible and efficient rlhf framework. *arXiv preprint arXiv:2409.19256*, 2024.
- [Sheng *et al.*, 2025] Guangming Sheng, Yuxuan Tong, Borui Wan, Wang Zhang, Chaobo Jia, Xibin Wu, Yuqi Wu, Xiang Li, Chi Zhang, Yanghua Peng, Haibin Lin, Xin Liu, and Chuan Wu. Laminar: A scalable asynchronous rl post-training framework, 2025.
- [Shoeybi *et al.*, 2019] Mohammad Shoeybi, Mostofa Patwary, Raul Puri, Patrick LeGresley, Jared Casper, and Bryan Catanzaro. Megatron-lm: Training multi-billion parameter language models using model parallelism. *arXiv preprint arXiv:1909.08053*, 2019.
- [Team and others, 2024] Qwen Team et al. Qwen2 technical report. *arXiv preprint arXiv:2407.10671*, 2(3), 2024.
- [Wei *et al.*, 2022] Jason Wei, Xuezhi Wang, Dale Schuurmans, Maarten Bosma, Fei Xia, Ed Chi, Quoc V Le, Denny Zhou, et al. Chain-of-thought prompting elicits reasoning in large language models. *Advances in neural information processing systems*, 35:24824–24837, 2022.
- [Wu *et al.*, 2025] Bo Wu, Sid Wang, Yunhao Tang, Jia Ding, Eryk Helenowski, Liang Tan, Tengyu Xu, Tushar Gowda, Zhengxing Chen, Chen Zhu, Xiaocheng Tang, Yundi Qian, Beibei Zhu, and Rui Hou. Llamarl: A distributed asynchronous reinforcement learning framework for efficient large-scale llm training, 2025.
- [Yang *et al.*, 2025] An Yang, Anfeng Li, Baosong Yang, Beichen Zhang, Binyuan Hui, Bo Zheng, Bowen Yu, Chang Gao, Chengen Huang, Chenxu Lv, et al. Qwen3 technical report. *arXiv preprint arXiv:2505.09388*, 2025.
- [Yao *et al.*, 2023] Zhewei Yao, Reza Yazdani Aminabadi, Olatunji Ruwase, Samyam Rajbhandari, Xiaoxia Wu, Ammar Ahmad Awan, Jeff Rasley, Minjia Zhang, Conglong Li, Connor Holmes, Zhongzhu Zhou, Michael Wyatt, Molly Smith, Lev Kurilenko, Heyang Qin, Masahiro Tanaka, Shuai Che, Shuaiwen Leon Song, and Yuxiong He. DeepSpeed-Chat: Easy, Fast and Affordable RLHF Training of ChatGPT-like Models at All Scales. *arXiv preprint arXiv:2308.01320*, 2023.
- [Zhang and Math-AI, 2024] Yifan Zhang and Team Math-AI. American invitational mathematics examination (aime) 2024, 2024.